Inorganica Chimica Acta 390 (2012) 53–60

Contents lists available at SciVerse ScienceDirect

Inorganica Chimica Acta

journal homepage: www.elsevier.com/locate/ica

Anion mediated diversity in the H-bonded assembly of a series of heteronuclear copper(II)/sodium(I) compounds

Prasanta Bhowmik [a], Subrata Jana [a], Partha Pratim Jana [b], Klaus Harms [b], Shouvik Chattopadhyay [a,*]

[a] Department of Chemistry, Inorganic Section, Jadavpur University, Kolkata 700032, India
[b] Fachbereich Chemie, Philipps-Universität Marburg, Hans-Meerwein-Straße, 35032 Marburg, Germany

ARTICLE INFO

Article history:
Received 1 December 2011
Received in revised form 21 February 2012
Accepted 23 March 2012
Available online 4 April 2012

Keywords:
Heteronuclear Cu(II)/Na(I)
Compartmental Schiff base
H-bonded architecture
Cyclic voltammetry

ABSTRACT

Three heteronuclear Cu(II)/Na(I) compounds, [Cu(vanpn)Na(NO_3)(H_2O)] (**1**), [Cu(vanpn)Na(N_3)(CH_3OH)] (**2**) and [Cu(vanpn)Na(NCS)(H_2O)] (**3**) where H_2vanpn = *N*,*N*′-(1,3-propylene)-bis(3-methoxysalicylideneimine), a well known compartmental Schiff base ligand, have been prepared and characterized by elemental analysis, IR and UV–Vis spectroscopy and single crystal X-ray diffraction studies. Compound **1** crystallises in monoclinic space group $P2_1/n$, compound **2** in triclinic $P\bar{1}$ and compound **3** in orthorhombic space group *Pbca*. In all the compounds, Cu atoms assume distorted square planar geometries whereas Na atoms exhibit distorted octahedral geometry. In compound **1**, the nitrate ion is coordinated as a chelating ligand and essentially both the O atoms of the nitrate occupy one axial site. Variation of the counter anions leads to considerable change in the H-bonded supramolecular structures of the compounds. Compound **1** forms a dimer, compound **2** constitutes a chain and compound **3** forms a helix. Electrochemical electron transfer study reveals Cu(II)Cu(I) reduction in acetonitrile solution.

1. Introduction

Supramolecular systems based on coordination compounds have received much attention because of their potential use as sensors, probes, photonic devices, and catalysts and in host–guest chemistry [1–7]. A significant number of supramolecular metal complexes have been synthesized in the last several years [8–12]. The two most commonly used approaches for engineering the crystal structure of such complexes employ either coordinative bonds [13–15] or hydrogen bonds [16–18]. Both approaches and their combinations have resulted in the construction of predesigned 2D or 3D supramolecular architectures. Hydrogen bonds have attracted considerable interest due to their relative strength, directionality, and ability to act synergically, thus providing a directing force for the organization of individual molecules into well-defined supramolecular assemblies. In this regard, it seemed interesting to conduct a systematic investigation on a designed series of transition metal complexes with the intention to understand the way in which H-bonding interactions cooperate and direct the supramolecular assembly of the molecular building blocks.

Structural studies have focused strongly on crown ethers, cryptands, and related ligands. Although these are particularly good classes of complexing agents for alkali metal ions, there are many other simpler and certainly more affordable ligands that are also extremely effective in this respect. One such ligand is H_2vanpn {=*N*,*N*′-(1,3-propylene)-bis(3-methoxysalicylideneimine)}, produced by the condensation of 3-methoxysalicaldehyde and 1,3-diaminopropane. This compartmental Schiff base has already been used exhaustively to prepare heterometallic 3d/4f compounds [19]. Structure determination showed that the 3d metals were placed in the N_2O_2 compartment of the ligand whereas lanthanide ions were placed in the O_2O_2 compartment in all the compounds without exception. Interestingly, reports on the preparation of 3d/alkali metal compounds with this ligand are relatively scanty and to the best to our knowledge, only three compounds are reported in the literatures which contain a transition metal and Na [20]. Of these three compounds, one is Cd/Na compound and the other two are Ni/Na compounds. No heteronuclear Cu/Na compounds with this ligand were reported in the literature till date. Furthermore, there is only one report of the preparation of Cu/alkali metal compound with this ligand in the CSD, where the alkali metal is potassium [21]. The diversity in the H bonding assembly of such 3d/alkali metal compounds with varying counter anions were also not studied systematically before the present work. Herein, we report the facile syntheses, crystal structures, spectroscopic and electrochemical studies and Hirshfeld analyses of three new heteronuclear Cu/Na compounds.

* Corresponding author. Tel.: +91 9903756480.
E-mail address: shouvik.chem@gmail.com (S. Chattopadhyay).

0020-1693/$ - see front matter © 2012 Elsevier B.V. All rights reserved.
http://dx.doi.org/10.1016/j.ica.2012.03.044

2. Experimental

2.1. Materials

All starting materials were commercially available, reagent grade, and used as purchased without further purification.

2.2. Synthesis

2.2.1. Synthesis of the ligand N,N′-propylene-bis(3-methoxysalicylideneimine) (H_2vanpn)

The hexadentate Schiff base ligand, H_2*vanpn*, was synthesized by refluxing 1,3-diaminopropane (10 mmol, 0.84 mL) with 3-methoxysalicyldehyde (20 mmol, 3.04 g) in methanol (20 ml) for ca. 1 h.

2.2.2. Synthesis of [Cu(vanpn)Na(NO_3)(H_2O)] (**1**)

A methanol solution (15 ml) of Cu(II) acetate monohydrate (1 mmol, 0.2 g) was added to the methanol solution (15 ml) of H_2*vanpn* (1 mmol, 0.342 g) and refluxed for 1 h. A solution of sodium nitrate (1 mmol, 0.085 g) in water (5 ml) was then added to it and stirred for 15 min. A green colored compound was precipitated out and was recrystallized from acetonitrile solution to obtain prismatic dark green single crystals suitable for X-ray diffraction.

Yield: 0.34 g (67%). *Anal.* Calc. for $C_{19}H_{22}CuN_3NaO_8$ (506.93): C, 45.02; H, 4.37; N, 8.29; Found: C, 45.4; H, 4.8; N, 8.3%. IR (KBr, cm^{-1}): 1598 ($\gamma_{C=N}$), 1468 (γ_{NO3}). UV–Vis, λ_{max} (nm) (ε_{max} ($dm^3\ mol^{-1}\ cm^{-1}$)) (acetonitrile), 609 (175), 375 (4616), Magnetic moment = 1.72 BM.

2.2.3. Synthesis of [Cu(Vanpn)Na(N_3)(CH_3OH)] (**2**)

It was prepared in a similar method to that of compound **1**, except that a solution of sodium azide (1 mmol, 0.065 g) in water (5 ml) was used instead of sodium nitrate. X-ray diffraction quality single crystals were obtained from the filtrate by slow evaporation in air.

Yield: 0.37 g (74%). *Anal.* Calc. for $C_{20}H_{24}CuN_5NaO_5$ (500.98): C, 47.95; H, 4.83; N, 13.98; Found: C, 47.9; H, 4.8; N, 13.6%. IR (KBr, cm^{-1}): 1615 ($\gamma_{C=N}$), 2044 (γ_{N3}). UV–Vis, λ_{max} (nm) (ε_{max} ($dm^3\ mol^{-1}\ cm^{-1}$)) (acetonitrile), 552 (290), 370 (3912), Magnetic moment = 1.71 BM.

2.2.4. Synthesis of [Cu(Vanpn)Na(NCS)(H_2O)] (**3**)

To prepare compound **3**, the acetonitrile solution (10 ml) of Cu(II) acetate monohydrate (1 mmol, 0.2 g) was added to the acetonitrile solution (10 ml) of H_2*vanpn* (1 mmol, 0.342 g) and refluxed for 1 h and a solution of sodium thiocyanate (1 mmol, 0.081 g) in water (5 ml) was then added to it. The mixture was stirred for about half an hour and filtered to remove a small amount of precipitate that appeared immediately. The filtrate was left at room temperature. Diffraction quality single crystals were obtained by slow evaporation of the filtrate in open atmosphere.

Yield: 0.36 g (71.6%). *Anal.* Calc. for $C_{20}H_{22}CuN_3NaO_5S$ (503): C, 47.76; H, 4.41; N, 8.35; Found: C, 47.8; H, 4.4; N, 8.6%. IR (KBr, cm^{-1}): 1620 ($\gamma_{C=N}$), 2079 (γ_{NCS}). UV–Vis, λ_{max} (nm) (ε_{max} ($dm^3\ mol^{-1}\ cm^{-1}$)) (acetonitrile), 565 (124), 366 (4557), Magnetic moment = 1.72 BM.

2.3. Physical measurements

Elemental analysis (carbon, hydrogen, and nitrogen) was performed using a Perkin–Elmer 240C elemental analyzer. IR spectra in KBr (4500–500 cm^{-1}) were recorded using a Perkin–Elmer RXI FT-IR spectrophotometer. Electronic spectra in acetonitrile (1200–350 nm) were recorded in a Hitachi U-3501 spectrophotometer. Electrochemical measurements were performed in acetonitrile solution under a dry nitrogen atmosphere in conventional three-electrode configurations using a Pt diskworking electrode, Pt auxiliary electrode and Ag/AgCl reference electrode, with tetrabutylammonium hexafluorophosphate as supporting electrolyte in the potential range from −2 to 2 V, and were uncorrected for junction contribution. The value for the Fc–Fc+ couple under our conditions is 0.5 V. The magnetic susceptibility measurements were done with an EG & PAR vibrating sample magnetometer, model 155 at room temperature and diamagnetic corrections were made using Pascal's constants.

2.4. X-ray crystallography

Crystals of compounds **1** and **3** were mounted in inert oil and transferred to the cold gas stream of the cooling device. Data have been collected at 193 K on a STOE IPDS (**1**) or at 100 K on a STOE IPDS 2T diffractometer (**3**) using graphite monochromated Mo Kα radiation, and have been corrected for absorption effects using multiscanned reflections (**1**, **3**). Non-hydrogen atoms were refined anisotropically. C bonded hydrogen atoms have been included on calculated positions and refined using the 'riding model'. O bonded hydrogens were located and refined isotropically. Programs used: SIR92 [22], SHELXL-97 [23,24], PLATON [25], and XAREA [26].

On the other hand, single crystals of **2** having suitable dimensions for the compound was used for data collection using a 'Bruker SMART APEX II' diffractometer equipped with graphite-monochromated Mo Kα radiation (λ = 0.71073 Å) at 293 K. The molecular structure was solved by direct methods and refinement by full-matrix least squares on F^2 using the SHELX-97 package [25,26]. Non-hydrogen atoms were refined with anisotropic thermal parameters. H atoms of water molecules were located by difference Fourier maps and were kept fixed. All other

Table 1
Crystal data and refinement details of compounds **1**–**3**.

	Compound **1**	Compound **2**	Compound **3**
Formula	$C_{19}H_{22}CuN_3NaO_8$	$C_{20}H_{24}CuN_5NaO_5$	$C_{20}H_{22}CuN_3NaO_5S$
Formula weight	506.93	500.98	503
Crystal size (mm)	0.26 × 0.24 × 0.21	0.3 × 0.2 × 0.2	0.10 × 0.08 × 0.05
T (K)	193	293	100
Crystal system	monoclinic	triclinic	orthorhombic
Space group	$P2_1/n$	$P\bar{1}$	$Pbca$
a (Å)	7.0672(10)	7.2590(2)	13.1161(4)
b (Å)	24.537(2)	11.0904(3)	13.6814(5)
c (Å)	12.0489(17)	13.5757(3)	24.0413(8)
α (°)	–	96.854(1)	–
β (°)	98.579(17)	101.099(1)	–
γ (°)	–	93.095(1)	–
Z	4	2	8
d_{calc} (g cm^{-3})	1.630	1.567	1.549
μ (mm^{-1})	1.132	1.093	1.167
F(000)	1044	518	2072
Total reflections	17321	15802	23177
Unique reflections	3648	15 287	3803
Observed data [$I > 2\sigma(I)$]	2654	10031	2716
No. of parameters	308	300	290
R_{int}	0.0641	0.0374	0.0688
$R1$, $wR2$ (all data)	0.0538, 0.0675	0.0749,0.1245	0.0755, 0.0637
$R1$, $wR2$ [$I > 2\sigma(I)$]	0.0318, 0.0632	0.0417, 0.1095	0.0408, 0.0569

hydrogen atoms were placed in their geometrically idealized positions and constrained to ride on their parent atoms. Empirical absorption corrections were carried out with the ABSPACK program [27]. A summary of the crystallographic data are given in Table 1. CCDC reference numbers are 841558 (for **1**), 837600 (for **2**) and 841559 (for **3**).

2.5. Hirshfeld surface analysis

Hirshfeld surfaces [28–30] and the associated 2D-fingerprint [31–33] plots were calculated using CrystalExplorer [34] which accepts a structure input file in CIF format. Bond lengths to hydrogen atoms were set to standard values. For each point on the Hirshfeld isosurface, two distances d_e, the distance from the point to the nearest nucleus external to the surface and d_i, the distance to the nearest nucleus internal to the surface, are defined. The normalized contact distance (d_{norm}) based on d_e and d_i is given by

$$D_{norm} = \frac{(d_i - r_i^{vdw})}{r_i^{vdw}} + \frac{(d_e - r_e^{vdw})}{r_e^{vdw}}$$

where r_i^{vdW} and r_e^{vdW} are the van der Waals radii of the atoms. The value of d_{norm} is negative or positive depending on intermolecular contacts being shorter or longer than the van der Waals separations. The parameter d_{norm} displays a surface with a red–white–blue color scheme, where bright red spots highlight shorter contacts white areas represent contacts around the van der Waals separation, and blue regions are devoid of close contacts. For a given crystal structure and set of spherical atomic electron densities, the Hirshfeld surface is unique [35], and it is this property that suggests the possibility of gaining additional insight into the intermolecular interaction of molecular crystals.

3. Results and discussion

3.1. Syntheses

The ligand (*H₂vanpn*) was prepared by the 1:2 condensation of the 1,3-diaminopropane with 3-methoxysalicyldehyde in methanol following the literature method [36]. *H₂vanpn* was then made to react with Cu(II) acetate monohydrate and stirring with sodium azide to prepare compound **1**. Compounds **2** and **3** were produced similarly by using sodium thiocyanate and sodium nitrate, respectively, instead of sodium azide. It is to be noted that in absence of any Na salt, [Cu(vanpn)(OH_2)] is produced where Cu(II) assumes a square pyramidal geometry. The X-ray structure of this compound is reported elsewhere [37]. This compound can also be used as the starting material in producing compounds **1**–**3** (Scheme 1). The coordinated water in the compound [Cu(vanpn)(OH_2)] is involved in H-bonding with the methoxy oxygen of a second, thereby forming a H-bonded dimer. When Na(I) is incorporated in the system, the geometry of Cu(II) ion is changed from square pyramidal to square planar. The H-bonding framework changes drastically on the incorporation of Na(I) in the O_4 compartment of the hexadentate Schiff Base. The formation of compounds **1**–**3** is shown in Scheme 1. [Cu(vanpn)(OH_2)] can also be prepared by refluxing $Cu(ClO_4)_2{\cdot}6H_2O$ with *H₂vanpn* in 1:1 ratio. It is very important to maintain the metal:ligand ratio in this synthetic procedure, because, on refluxing $Cu(ClO_4)_2{\cdot}6H_2O$ with *H₂vanpn* in 3:2 ratio, a tri-nuclear compound [Cu(vanpn)Cu(vanpn)Cu](ClO_4)$_2$ was produced, the structure of which is reported by a different group [38]. Once this tri-nuclear compound is formed, heteronuclear Cu(II)/Na(I) compounds could not be prepared.

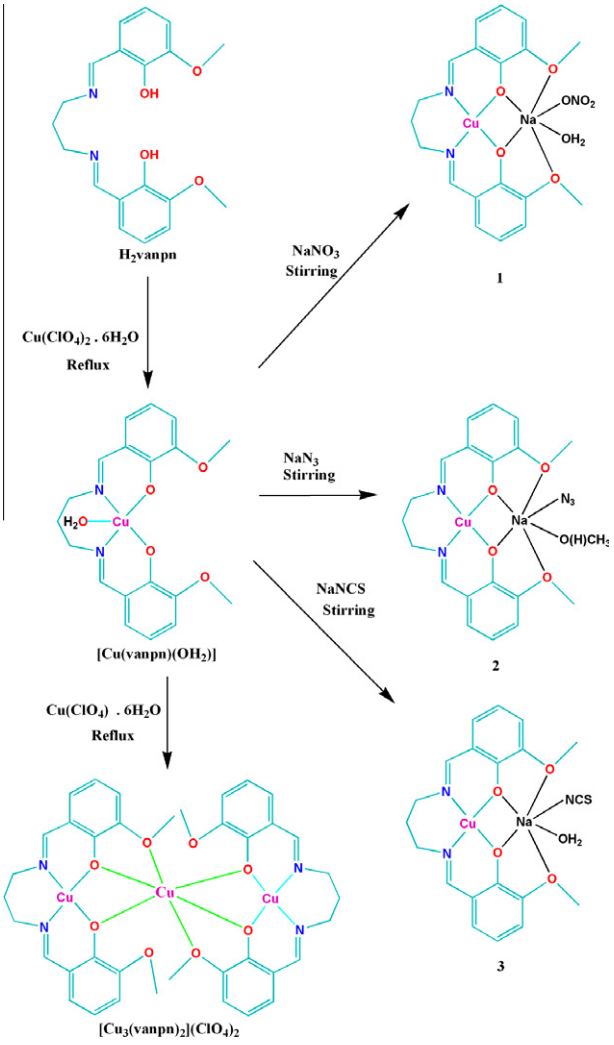

Scheme 1. Formation of the compounds.

3.2. Description of structures

3.2.1. [Cu(vanpn)Na(NO_3)(H_2O)] (*1*)

The molecular structure of **1** is built from isolated dinuclear molecules of [Cu(vanpn)Na(NO_3)(H_2O)]. A perspective view of this compound with the corresponding labeling scheme is depicted in Fig. 1. This structure is very similar to the analogous 3d–4f Schiff base compounds studied earlier [39,40]. In each bimetallic unit, the Cu(II) and Na(I) atoms occupy the inner N_2O_2 and outer O_2O_2 sites, respectively. The coordinating atoms N(8), N(12), O(1) and O(3), deviate 0.236(2), −0.234(2), −0.283(2) and 0.280(2) Å, respectively from the mean square plane and the Cu(II) atom is 0.015 Å away from the same plane. The conformation of the saturated six-membered ring {Cu(1)–N(8)–C(9)–C(10)–C(11)–N(12)} is closer to screw boat with the puckering parameters [41,42] $Q = 0.643(3)$ Å, $\theta = 67.95(18)°$, $\varphi = 151.1(2)°$. The N(8)–Cu(1)–N(12) angle is 97.57(9)° and is typical of six-membered chelate [43]. Cu(II) and Na(I) are doubly bridged to each other by two phenoxo oxygen atoms, O(1) and O(3), with Cu(1)···Na(1) distance of 3.462(12) Å. The Na(I) is surrounded by four oxygen atoms, O(1), O(2), O(3), and O(4) of the Schiff base and a oxygen atom, O(100) of water moiety and two O atoms, O(11) and O(12) of the nitrate. The small value (50.5°) of the angle [O(11)–Na(1)–O(12)], subtended by the two O atoms at the metal, traces on the point that the two oxygen atoms are sharing one axial site, i.e. the nitrate group

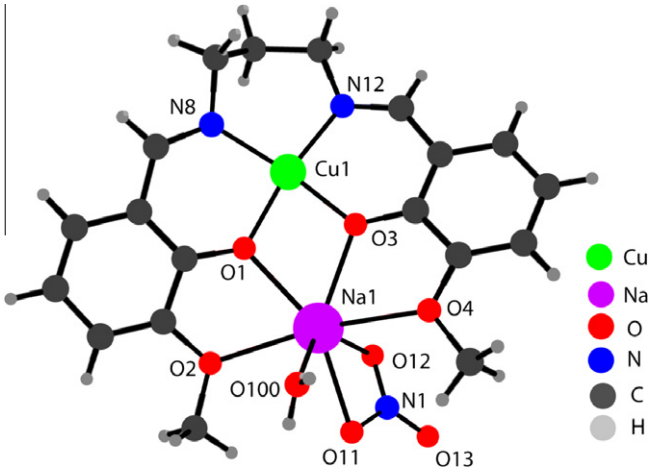

Fig. 1. Perspective view of compound **1** along with the atom numbering of all non-carbon non-hydrogen atoms. Disordered oxygen atom is not shown for clarity. Selected bond distances (Å): Cu(1)–N(8) 1.944(2), Cu(1)–N(12) 1.978(2), Cu(1)–O(1) 1.917(17), Cu(1)–O(3) 1.8993(18), l Na(1)–O(1) 2.385(2), Na(1)–O(2) 2.515(2), Na(1)–O(3) 2.357(2), Na(1)–O(4) 2.552(2), Na(1)–O(11) 2.505(2), Na(1)–O(12) 2.488(15), Na(1)–O(100) 2.352(2). Bond angles are given in Supplementary Table S1.

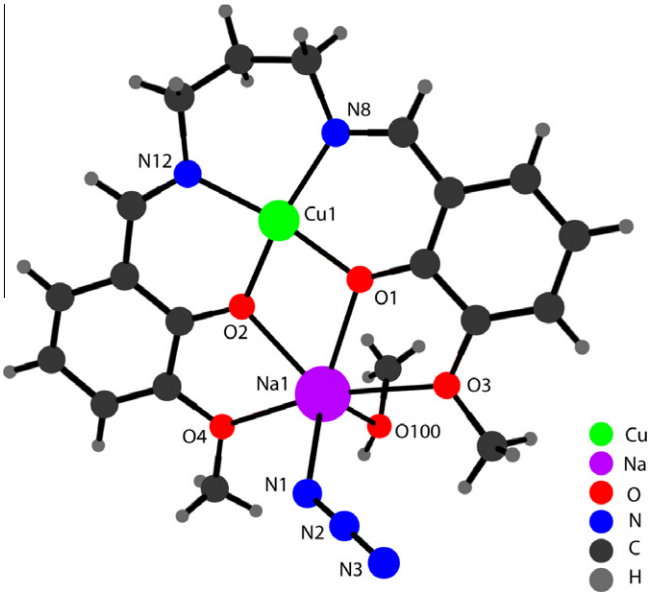

Fig. 2. Perspective view of compound **2** showing the atom numbering of relevant atoms. Selected bond distances (Å): Cu(1)–N(8) 1.9934(10), Cu(1)–N(12) 1.9664(9), Cu(1)–O(1) 1.9184(8), Cu(1)–O(2) 1.9181(8), Na(1)–O(3) 2.4602(11), Na(1)–O(1) 2.3743(9), Na(1)–O(4) 2.4479(11), Na(1)–O(2) 2.3375(9), Na(1)–O(100) 2.3894(15), Na(1)–N(1) 2.4118(17) Bond angles are given in Supplementary Table S2.

is better thought of as a single entity occupying just one stereochemical site in the coordination sphere of the metal instead of as a bidentate ligand. Thus the geometry around the Na atom is distorted octahedral. The bridging angles Cu(1)–O(1)–Na(1) and Cu(1)–O(3)–Na(1) are 106.65(8) and 108.38(8) respectively. The dihedral angle between the Cu(1)O(1)O(2) and O(1)O(2)Na(1) planes is equal to 1.65°. The Cu(1)O(1)O(2)Na(1) core is thus planar. The distance of Na–O(methoxy) is also larger than that of Na–O(phenolate). The selected bond lengths and bond angles are given in Table S1.

3.2.2. [Cu(vanpn)Na(N_3)(CH_3OH)] (**2**)

The structure determination reveals that the compound crystallizes in the triclinic space group $P\bar{1}$ with the asymmetric unit consisting of heteronuclear compound [Cu(vanpn)Na(N_3)(CH_3OH)]. A structural diagram is shown in Fig. 2. This structure is very similar to that of compound **1**. In each bimetallic unit, the Cu(II) and Na(I) atoms occupy the inner N_2O_2 and outer O_2O_2 sites, respectively. The distortion of the coordinating atoms N(8), N(12), O(1) and O(2) from the least-square mean plane through them are −0.108(1), 0.108(1)–0.130(1) and −0.129(1) Å, respectively, and that of Cu atom from the same plane is 0.026 Å. The conformation of the saturated six-membered ring {Cu(1)–N(8)–C(9)–C(3)–C(2)–N(12)} is in between screw boat and envelope with the puckering parameters 53 $Q = 0.5845(14)$ Å, $\theta = 116.53(12)°$, $\varphi = 18.17(14)°$. The N(8)–Cu(1)–N(12) angle is 96.74(4)° and is typical of six-membered chelate [43]. The Na(I) is octahedrally surrounded by NO5 moiety. The two phenoxo oxygen atoms, O(1) and O(2), two methoxy oxygen atoms, O(3) and O(4) of the deprotonated di-Schiff base constitute the equatorial plane around Na(I). O(100) from a methanol and N(1) from an azide are coordinated in the axial positions. The two different geometries of Cu and Na share a common edge defined by the bridging phenolate oxygen atoms O(1) and O(2). The bridging Na–O(phenolate) bonds (av. 2.355 Å) are longer than the Na–O(phenolate) bonds (av.1.918 Å). Also the Na–O(methoxy) distances (av. 2.454 Å) are larger than that of Na–O(phenolate). The intra-molecular Cu(1)···Na(1) distance is 3.463 Å. The bridge angles Cu(1)–O(1)–Na(1) and Cu(1)–O(2)–Na(1) are 107.08(4)° and 108.53(4)°, respectively. The Cu(1)O(2)O(3)Na(1) core is almost planar, the dihedral angles between the O(2)Cu(1)O(3) and O(2) Na(1)O(3) planes being 6.830. The selected bond lengths and bond angles are given in Table S2.

3.2.3. [Cu(vanpn)Na(NCS)(H_2O)] (**3**)

Compound **3** crystallises in the orthorhombic space group *Pbca*. The molecular structure of **3** in Fig. 3 reveals a heteronuclear compound which is similar to that in compounds **1** and **2** with the coordination of thiocyanate to Na(I) instead of nitrate (as in **1**) or azide (as in **2**). Cu(1) has a four-coordinate distorted square planner geometry in which O(1), O(2), N(8), and N(12) atoms of deprotonated di-Schiff base $(vanpn)^{2-}$ constitute the equatorial plane. There is a slight distortion to the square plane and the deviations of the coordinating atoms N(8), N(12), O(1), and O(2) from the least-square mean plane through them are −0.152(3), 0.153(3), 0.183(2) and −0.184(2) Å, respectively, and that of Cu atom from the same plane is 0.045 Å. The conformation of the saturated six-membered ring {Cu(1)–N(8)–C(9)–C(10)–C(11)–N(12)} is closer to envelope with the puckering parameters $Q = 0.566(4)$ Å, $\theta = 125.4(3)°$, $\varphi = 348.9(4)°$ [44,45]. The N(8)–Cu(1)–N(12) angle is 97.29(10)° and is typical of six-membered chelate [44,45]. The coordination environment around Na(I) shows a distorted octahedral geometry involving O2O2 donors in the basal plane {phenoxo oxygen atoms, O(1) and O(2); and methoxy oxygen atoms, O(3) and O(4)}. One oxygen atom, O(100), from a water molecule and one nitrogen atom, N(1), from a thiocyanate, are attached to the sodium to fill its two axial sites. The distance of Na–O(methoxy) is larger than that of Na–O(phenolate). The Cu(1)···Na(1) intra-molecular distance is 3.479(11) Å. The bridge angles Cu(1)–O(1)–Na(1) and Cu(1)–O(2)–Na(1) are 107.18(9)° and 108.34(9)°, respectively. The Cu(1)O(1)O(2)Na(1) core is almost planar, the dihedral angles between the O(1)Cu(1)O2) and O(1) Na(1)O(2) planes being 5.130. The selected bond lengths and bond angles are given in Table S2.

3.2.4. H bonded network in compounds **1**–**3**

The hydrogen atom, H(101), attached with O(100) of the coordinated water molecule in **1** is engaged in hydrogen bond formation with the symmetry related (# = 2 − *x*, 1 − *y*, 2 − *z*) oxygen atom,

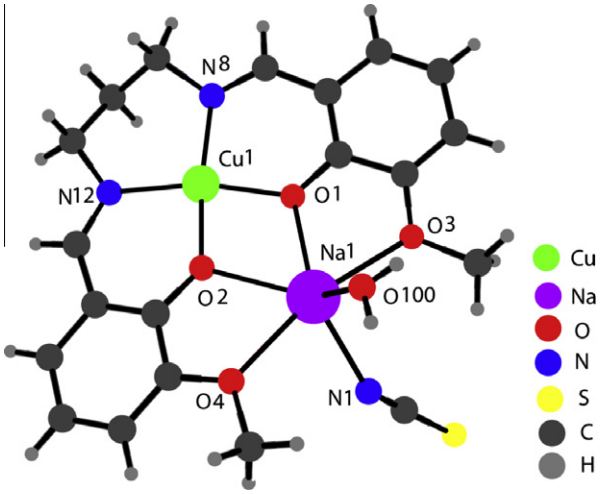

Fig. 3. Perspective view of compound **3**. Selected bond distances (Å): Cu(1)–N(8) 1.977(3), Cu(1)–N(12) 1.989(2), Cu(1)–O(1) 2.427(3), Cu(1)–O(2) 1.920(2), Na(1)–O(1) 2.383(2), Na(1)–O(2) 2.359(2), Na(1)–O(3) 2.471(2), Na(1)–O(4) 2.448(3), Na(1)–O(100) 2.310(3), Na(1)–N(1) 1.9267(18). Selected bond distances (Å): Bond angles are given in Supplementary Table S2.

O(11), to form a dimer (Fig. 4). In this dimer, a chair is formed by Na(1), O(11), O(100) and their symmetry-related counter parts. In compound **2**, the hydrogen atom, H(39), attached with O(100) of the coordinated methanol molecule is engaged in hydrogen bond formation with the symmetry related ($*$ = 1 + x, y, z) nitrogen atom, N(3) to form a chain (Fig. 5). S atom of NCS ligand in compound **3** is hydrogen-bonded with the symmetry related hydrogen atoms (u = $-1/2 + x$, $1/2 - y$, $2 - z$ and v = $1/2 - x$, $-1/2 + y$, z) of the water moiety of another molecule of same compound to form helical structure (Fig. 6). The details of H bonding are given in Table 2.

3.3. Hirshfeld surfaces

The Hirshfeld surfaces of the compounds are illustrated in Fig. S1, showing surfaces that have been mapped over a d_{norm} (range of −0.5 to 1.5 Å), shape index and curvedness. The surfaces are shown as transparent to allow visualization of the molecular moiety, in a similar orientation for all structures, around which they were calculated.

The dominant interactions between N···H, O···H and S···H atoms in the compounds **1**–**3** can be seen in the Hirshfeld surface as the red areas in Fig. S1. Other visible spots in the Hirshfeld surfaces correspond to H···H contacts. The small extent of area and light color on the surface indicates weaker and longer contact other than hydrogen bonds. The O···H/H···O intermolecular interactions appear as distinct spikes in the 2D fingerprint plot for compound **1** (Fig. S2). The N···H and S···H intermolecular interactions appear as two distinct spikes in the 2D fingerprint plots (Fig. S3), in compounds **2** and **3**, respectively. Complementary regions are visible in the fingerprint plots where one molecule act as donor ($d_e > d_i$) and the other as an acceptor ($d_e < d_i$). The fingerprint plots can be decomposed to highlight particular atoms pair close contacts. This decomposition enables separation of contributions from different interaction types, which overlap in the full fingerprint. The proportion of O···H/H···O interaction are comprising of 33.0% of the Hirshfeld surfaces for each molecule of compound **1**. The O···H interaction is represented by a spike (d_i = 0.756, d_e = 1.102 Å in compound **1**) in the bottom left (donor) area of the fingerprint plot (Fig. S2), indicating H-atoms of H_2O molecule are interacting with O-atom of the nitrate/acetate group. The H···O interaction is also represented by another spike (d_e = 0.756, d_i = 1.102 Å in compound **1**) in the bottom right (acceptor) region of fingerprint plot, where nitrate/acetate oxygen also acts as acceptor to the H atoms of the H_2O molecule and these oxygen-based interactions represent the closest contacts in the structures and can be viewed as a pair of large red spots on the d_{norm} surface (Fig. S1a). The proportion of N···H/H···N interactions comprises 20.40% of the Hirshfeld surfaces for each molecule of compound **2**. The N···H interactions are represented by a spike (d_i = 0.746, d_e = 1.127 Å) in the bottom left (donor) area of the fingerprint plot (Fig. S3a), indicating H-atoms of H_2O molecule are interacting with N-atom of the azide group. The H···N interactions are represented by another spike (d_e = 0.746, d_i = 1.127 Å) in the bottom right (acceptor) region of fingerprint plot (Fig. S3a), where azide nitrogen also acts as acceptor to the H atoms of the H_2O molecule and these nitrogen-based interactions represent the closest contacts in the structures and can be viewed as a pair of large red spots on the d_{norm} surface (Fig. S1b) The proportion of S···H/H···S interactions comprises 13.2% of the Hirshfeld surfaces for each molecule of compound **3**. The S···H interactions are represented by a spike (d_i = 0.866, d_e = 1.503 Å) in the bottom left (donor) area of the fingerprint plot (Fig. S3b), indicating H-atoms of H_2O molecule are interacting with S-atom of the thiocyanate group, whereas the H···S interactions are represented by another spike (d_e = 0.866, d_i = 1.503 Å) in the bottom right (acceptor) region of fingerprint plot (Fig. S3b), where thiocyanate sulfur acts as acceptor to the H atoms of the H_2O molecule and these sulfur-based interactions represent the closest contacts in the structures and can be viewed as a pair of large red spots on the d_{norm} surface (Fig. S1c). The relative contribution of the different interactions to the Hirshfeld surface was calculated for compounds **1**–**3** and some similar compounds (Fig. S4) available in the CSD.

3.4. IR and electronic spectra and magnetic properties

In the IR spectra of compounds **1**–**3**, distinct bands due to the azomethine (C=N) group within 1649–1573 cm^{-1} are customarily noticed [46]. Broad bands around 3400 cm^{-1} in IR spectra of compounds **1** and **3** are assigned to the OH stretching vibration of the coordinated water molecule, which is involved in hydrogen bonding [47]. The bands in the range of 2929–2930 cm^{-1} are due to alkyl C–H bond stretching of methoxy groups [48]. The presence as well as coordination mode of azide to a transition metal can be detected by the intense IR band due to νN_3 that usually appears within 2000–2055 cm^{-1} for terminal azide [49]. In the IR spectrum of **2**, the appearance of strong band at 2044 cm^{-1} indicates the presence of monodentate azide [50]. Similarly, a band at 2079 cm^{-1} in compound **3** is indicative of the presence of the N-coordinated thiocyanate where as twin bands at 1320 and 1468 cm^{-1} indicates unsymmetrical chelating nitrate group in compound **1** [50].

The electronic spectra in acetonitrile solution have been recorded for the three compounds. The appearance of two bands at 606 and 373 nm (compound **1**), 552 and 370 nm (compound **2**), 565 and 366 nm (compound **3**) in the absorption spectra are consistent with the square planar geometry of Cu(II) [51].

Room temperature magnetic susceptibility measurements show that all the compounds have magnetic moments close to 1.73 BM.

3.5. Thermo-gravimetric analysis

Thermo-gravimetric analyses of compounds **1** and **3** show a weight loss of ~3.75% and 3.85%, respectively in the temperature range 80–150 °C, which corresponds to the loss of one water molecule (Calc. 3.55%). Compound **2** shows a weight loss of ~7% in the temperature range 50–110 °C which corresponds to the loss of a

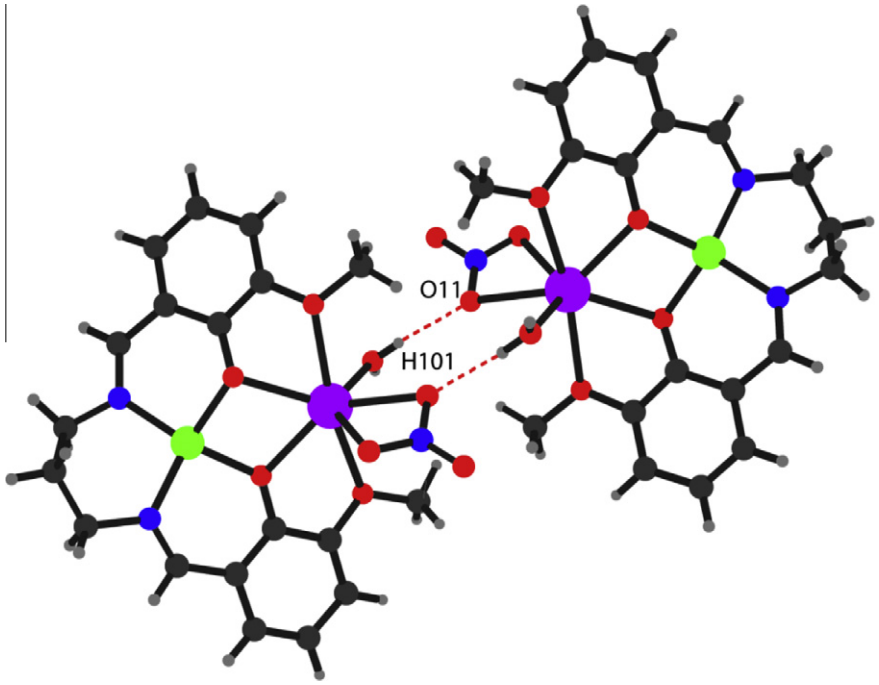

Fig. 4. H-bonded dimer of compound **1**.

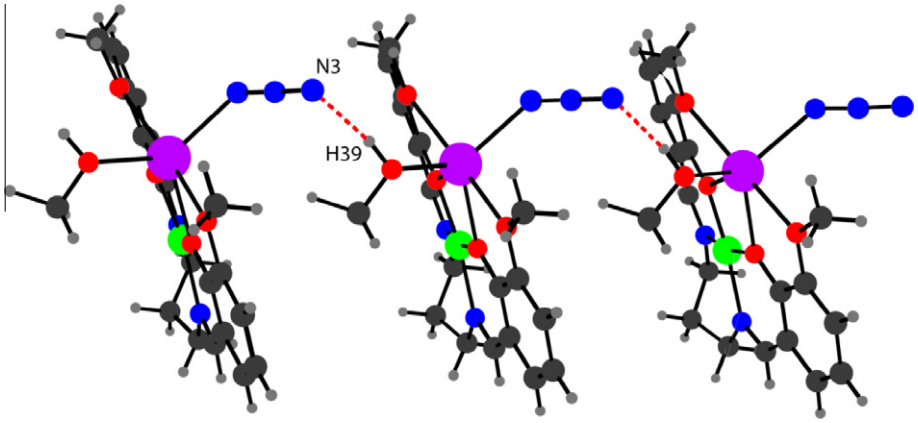

Fig. 5. H-bonded chain of compound **2**.

methanol molecule (Calc. 6.4%). The dehydrated species does not absorb any water molecules on exposure to open atmosphere. In the IR spectra of the dehydrated species, the broad band at ca. 3490 cm^{-1} is missing, confirming the elimination of the water molecule on heating.

3.6. Cyclic voltammetry

The redox properties of the Cu(II) compounds exhibit more or less similar features consisting of a reversible or quasi-reversible Cu(II)/Cu(I) reduction. The criteria of reversibility were checked by observing constancy of peak-peak separation ($\Delta E_p = E_{pa} - E_{pc}$) and the ratio of peak heights ($i_{pa}/i_{pc} \sim 1$) with variation of scan rates [52]. Only very few Cu(II)/Cu(I) couples exhibit truly reversible electrochemical behavior because Cu(II) has a tendency toward six-coordinate tetragonal geometries while Cu(I) appears to prefer four-coordinate tetrahedral geometries. The subsequent rearrangement of the Cu coordination sphere upon the reduction of the Cu(II) species typically leads to a relatively slow chemical reaction following the electron transfer process. Reversible behavior can only be seen in cases where the geometry of the Cu compound is essentially the same before and after the reduction. The only coordination number that is common to both oxidation states is four, and even in these systems Cu(I) may have regular tetrahedral coordination sphere but Cu(II) always involves a compressed tetrahedral or square planar geometry. In the present study, the compounds **1** and **2** exhibit reversible signals whereas compounds **3** exhibit quasi-reversible signals. The single-electron nature of the voltammograms has been confirmed by the comparison of current heights for the compounds and that of a simple $[Fe(bipy)_3]^{2+}$ compound under identical conditions [53]. It has been observed that no well defined oxidative or reductive responses could be observed on running further in the positive or negative potential. The $E_{1/2}$ and ΔE_p values for these redox couples are given in Table 3. All the redox signals remain virtually invariant under different scan rates (0.01–1.0 V s^{-1}) in the temperature range 300–280 K. Solvent dependent shift and change in electrochemical reversibility of redox couples are not significant.

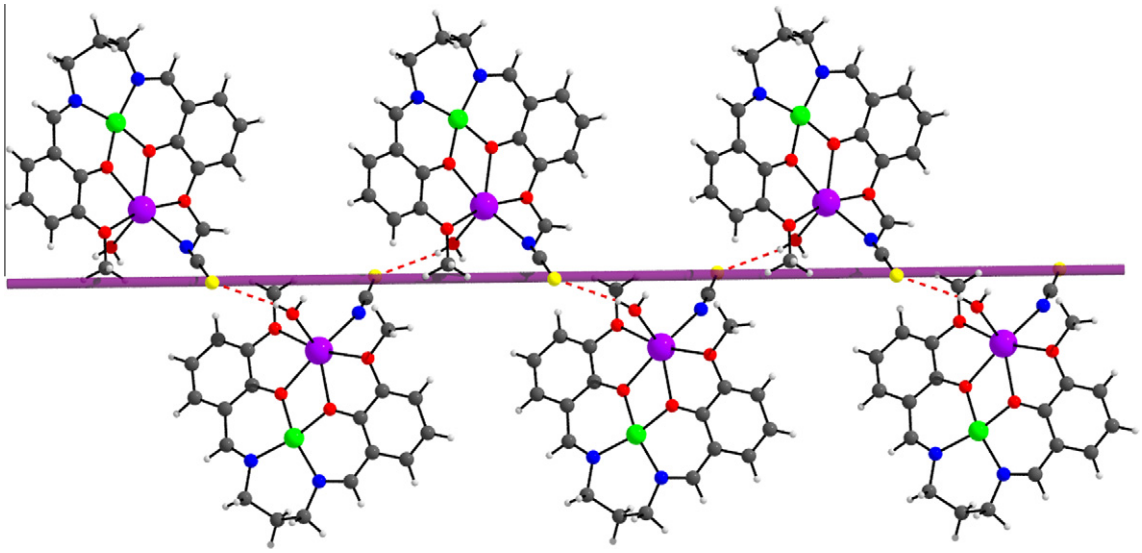

Fig. 6. H-bonded helix of compound **3**.

Table 2
H-bond distances in compounds **1**–**3**.

	D–H···A	D–H	D···A	H···A	∠D–H···A
1	O(100)–H(101)···O(11)$^{\#}$	0.81(4)	2.03(4)	2.834(3)	171(4)
2	O(100)–H(39)···N(3)*	0.89(3)	1.97(3)	2.844(2)	168(3)
3	O(100)–H(101)···S(1)^{u}	0.77(5)	2.59(5)	3.313(4)	158(4)
	O(100)–H(102)···S(1)^{v}	0.82(5)	2.54(5)	3.361(3)	173(5)

Symmetry element # = 2 − *x*, 1 − *y*, 2 − *z*, * = 1 + *x*, *y*, *z*, *u* = −1/2 + *x*, 1/2 − *y*, 2 − *z* and *v* = 1/2 − *x*, −1/2 + *y*, *z*.

Table 3
Electrochemical data for compounds **1**–**3**.

Compound	Cu(II)/Cu(I)			
	E_{pa} (V)	E_{pc} (V)	$E_{1/2}$ (V)	ΔE_p (mV)
1	−1.62	−1.68	−1.65	60
2	−1.54	−1.58	−1.56	40
3	−1.55	−1.63	−1.59	80

$E_{1/2}$ is calculated as the average of anodic (E_{pa}) and cathodic (E_{pc}) peak potentials; $\Delta E_p = (E_{pa} - E_{pc})$.

4. Conclusion

The syntheses and characterization of three iso-structural compounds [Cu(II)(vanpn)Na(I)X] (X = NO_3, N_3, NCS) with *N*,*N*′-propylenebis(3-ethoxysalicylaldiimine) (H_2vanpn) have been described in the present paper. It has been presented that the reaction of Cu(II)and Na(I) salts with a compartmental Schiff base can afford interesting heteronuclear compounds with different H-bonded supramolecular assembly varying from dimer to helical chain. The representative anions are applied to construct these H-bonded architectures. Thus, this work gives rise to a promising method for rationally designing and controlling structural assemblies of related coordination species.

Acknowledgements

This work was supported by CSIR, India (Fellowship for Prasanta Bhowmik, Sanction No. 09/096(0607)/2010-EMR-I, dated 27.1.10, and for Subrata Jana, Sanction No. 09/096(0659)/2010-EMR-I, dated 18.1.11) and University Grants Commission, CAS-UGC, New Delhi.

Appendix A. Supplementary material

Supplementary data associated with this article can be found, in the online version, at http://dx.doi.org/10.1016/j.ica.2012.03.044.

References

[1] J.M. Lehn, Angew. Chem., Int. Ed. Engl. 27 (1988) 89.
[2] H.J. Schneider, Angew. Chem., Int. Ed. Engl. 30 (1991) 1417.
[3] D.J. Braga, J. Chem. Soc., Dalton Trans. (2000) 3705.
[4] H. Li, M. Eddaoudi, M. O'Keeffe, O.M. Yaghi, Nature 402 (1999) 276.
[5] D.J. Stufkens, A. Vleck Jr., Coord. Chem. Rev. 177 (1998) 127.
[6] J.L. Atwood, J.E.D. Davies, D.D. MacNicol, F. Vogtle, J.M. Lehn, in: J.M. Lehn (Ed.), Comprehensive Supramolecular Chemistry, vol. vols. 6 and 9, Pergamon, Oxford, 1996.
[7] M.J. Blanco, M.C. Jimenez, J.C. Chambron, V. Heitz, M. Linke, J.P. Sauvage, Chem. Soc. Rev. 28 (1999) 293.
[8] M. Fujita, Chem. Soc. Rev. 27 (1998) 417.
[9] P.K. Iyer, J.B. Beck, C. Weder, S.J. Rowan, Chem. Commun. (2005) 319.
[10] G.R. Whittell, M.D. Hager, U.S. Schubert, I. Manners, Nat. Mater. 10 (2011) 176.
[11] M. Albrecht, Naturwissenschaften 94 (2007) 951.
[12] E. Pardo, R. Ruiz-García, J. Cano, X. Ottenwaelder, R. Lescoue'zec, Y. Journaux, F. Lloret, M. Julve, Dalton Trans. (2008) 2780.
[13] A.J. Blake, N.R. Champness, P. Hubberstey, W.S. Li, M.A. Withersby, M. Schro'der, Coord. Chem. Rev. 183 (1999) 117.
[14] R. Robson, Dalton Trans. (2000) 3735.
[15] B. Moulton, M.J. Zaworotko, Chem. Rev. 101 (2001) 1629.
[16] R.E. Mele'ndez, A.D. Hamilton, Top. Curr. Chem. 198 (1998) 97.
[17] C.B. Aakero'y, A.M. Beatty, Aust. J. Chem. 54 (2001) 409.
[18] A.D. Burrows, Struct. Bonding (Berlin) 108 (2004) 5595.
[19] CSD search file 1.pdf (Supporting Information).
[20] CSD search file 2.pdf (Supporting Information).
[21] D.G. Branzea, A. Guerri, O. Fabelo, C. Ruiz-Perez, L.-M. Chamoreau, C. Sangregorio, A. Caneschi, M. Andruh, Cryst. Growth Des. 8 (2008) 941.
[22] A. Altomare, G. Cascarano, C. Giacovazzo, A. Guagliardi, J. Appl. Crystallogr. 26 (1993) 343.
[23] G.M. Sheldrick, Acta Crystallogr., Sect. A 64 (2008) 112.
[24] G.M. Sheldrick, SHELXS-97 and SHELXL-97, University of Göttingen, Germany, 1997.
[25] A.L. Spek, Acta Crystallogr., Sect. A 46 (1990) C34.
[26] X-AREA, version 1.56, STOE & Cie GmbH, Darmstadt, 2011.
[27] ABSPACK, version 1, Oxford Diffraction, Abingdon, 2005.
[28] M.A. Spackman, D. Jayatilaka, CrystEngCommun. 11 (2009) 19.
[29] F.L. Hirshfeld, Theor. Chim. Acta 44 (1977) 129.
[30] H.F. Clausen, M.S. Chevallier, M.A. Spackman, B.B. Iversen, New J. Chem. 34 (2010) 193.
[31] A.L. Rohl, M. Moret, W. Kaminsky, K. Claborn, J.J. McKinnon, B. Kahr, Cryst. Growth Des. 8 (2008) 4517.
[32] A. Parkin, G. Barr, W. Dong, C.J. Gilmore, D. Jayatilaka, J.J. McKinnon, M.A. Spackman, C.C. Wilson, CrystEngCommun. 9 (2007) 648.
[33] M.A. Spackman, J.J. McKinnon, CrystEngCommun. 4 (2002) 378.
[34] S.K. Wolff, D.J. Grimwood, J.J. McKinnon, D. Jayatilaka, M.A. Spackman, Crystal Explorer 2.0, University of Western Australia, Perth, Australia, 2007. <http://hirshfeldsurfacenet.blogspot.com/>.

[35] J.J. McKinnon, M.A. Spackman, A.S. Mitchell, Acta Crystallogr., Sect. B 60 (2004) 627.
[36] P. Bhowmik, H.P. Nayek, M. Corbella, N. Aliaga-Alcalde, S. Chattopadhyay, Dalton Trans. 40 (2011) 7916.
[37] S. Thakurta, J. Chakraborty, G. Rosair, R.J. Butcher, S. Mitra, Inorg. Chim. Acta 362 (2009) 2828.
[38] S. Thakurta, C. Rizzoli, R.J. Butcher, C.J. Gómez-García, E. Garribba, S. Mitra, Inorg. Chim. Acta 363 (2010) 1395.
[39] J.-P. Costes, F. Dahan, A. Dupuis, J.-P. Laurent, Inorg. Chem. 35 (1996) 2400.
[40] J.-P. Costes, F. Dahan, A. Dupuis, J.-P. Laurent, New J. Chem. (1998) 1525.
[41] D. Cramer, J.A. Pople, J. Am. Chem. Soc. 97 (1975) 1354.
[42] J.C.A. Boyens, J. Cryst. Mol. Struct. 8 (1978) 317.
[43] S. Chattopadhyay, M.G.B. Drew, A. Ghosh, Inorg. Chim. Acta 359 (2006) 4519 (and the references there in).
[44] I.R. Laskar, D. Das, G. Mostafa, T.H. Lu, T.C. Keng, J.C. Wang, A. Ghosh, N. Ray Chaudhuri, New J. Chem. 25 (2001) 764.
[45] I.R. Laskar, A. Ghosh, G. Mostafa, D. Das, A. Mondal, N. Ray Chaudhuri, Polyhedron 19 (2000) 1015.
[46] P. Bhowmik, S. Chattopadhyay, M.G.B. Drew, C. Diaz, A. Ghosh, Polyhedron 29 (2010) 2637 (and references there in).
[47] M.S. Ray, S. Chattopadhyay, M.G.B. Drew, A. Figuerola, J. Ribas, C. Diaz, A. Ghosh, Eur. J. Inorg. Chem. (2005) 4562.
[48] C.J. Cooper, M.D. Jones, S.K. Brayshaw, B. Sonnex, M.L. Russell, M.F. Mahon, D.R. Allan, Dalton Trans. 40 (2011) 3677.
[49] S.S. Tandon, L.K. Thompson, M.E. Manuel, J.N. Bridson, Inorg. Chem. 33 (1994) 5555.
[50] K. Nakamoto, Infrared Spectra of Inorganic Compounds, Wiley, New York, 1970.
[51] S. Chattopadhyay, M.S. Ray, S. Chaudhuri, G. Mukhopadhyay, G. Bocelli, A. Cantoni, A. Ghosh, Inorg. Chim. Acta 359 (2006) 1367.
[52] D.H. Evans, K.M. O'Connell, R.A. Petersen, M.J. Kelly, J. Chem. Educ. 60 (1983) 290.
[53] K. Mitra, S. Biswas, C.R. Lucas, B. Adhikary, Inorg. Chim. Acta 359 (2006) 1997.